Theoretical Study of the Conformational Isomerism of 2,4,6-Substituted 1,3,5-Trimethoxycalix[6]arenes

Willem P. van Hoorn, Frank C. J. M. van Veggel,* and David N. Reinhoudt*

Laboratory of SupraMolecular Chemistry and Technology, University of Twente, P.O. Box 217, 7500 AE Enschede, The Netherlands

Received: February 18, 1998; In Final Form: May 18, 1998

For 2,4,6-trisubstituted 1,3,5-trimethoxycalix[6]arenes **1**, two competing interconversion pathways have been postulated in the literature for the Cone/1,2,3Alternate exchange, viz the "*tert*-butyl through the annulus" and "lower rim through the annulus" pathways. Both pathways were compared with molecular modeling with the conjugate peak refinement method. One variable-size atom (Sx) was introduced to represent the lower-rim substituents R, abstracting the "O−CH_2−rigid group" motifs to one "O−CH_2−Sx" group. Both the postulated mechanisms of Cone → 1,2,3Alternate isomerization are plausible. For large lower-rim substituents (Sx ≥ ≈6 Å), the "*tert*-butyl through the annulus" mechanism is preferred over the "Sx through the annulus" mechanism. The calculated upper free energy barrier for the isomerization process is 17.5 kcal mol^{-1}, reasonably close to the experimental value of approximately 21 kcal mol^{-1} (van Duynhoven et al. *J. Am. Chem. Soc.* **1994**, *116*, 5814).

Introduction

Calix[4]arenes have proven to be useful building blocks in supramolecular chemistry, because of the possibility of selective functionalization and control over the conformation.[1] The selective functionalization of calix[6]arenes has recently been explored,[2] but in contrast to calix[4]arenes, it is difficult to immobilize the conformations of calix[6]arenes. The introduction of large lower-rim substituents[3−5] and various bridges[6,7] and caps[8,9] have yielded a small number of conformationally fixed calix[6]arenes. The difficulty in freezing the conformation of calix[6]arenes is illustrated by the 2,4,6-trisubstituted 1,3,5-trimethoxycalix[6]arenes **1** (Chart 1). Compound **1c** was presented as the first example of a calix[6]arene frozen in the Cone conformation,[10] but later it was shown[5,11] that all calix[6]arenes **1** exist as two slowly exchanging conformers. The major conformer is a C_{3v} Cone and the minor one is a C_s 1,2,3-Alternate (1,2,3Alt), as determined by 2D NMR in $CDCl_3$ and CD_2Cl_2 (Figure 1).[5] The stability of both conformations has been explained by self-inclusion of the methoxy moieties, which gives rise to attractive CH···p interactions.[5] The free energy differences between the stable conformers ($\Delta G°$) and the free energy changes of conformational exchange of **1** ($\Delta G^{\ddagger}$) have been determined (Table 1).[5]

The upper limit of the activation free energy barrier of ≈ 21 kcal mol^{-1} for large lower-rim substituents R has been explained by assuming that conformational interconversion can proceed via two different pathways, viz., the "*p-tert*-butyl through the annulus" and the "lower rim through the annulus" mechanisms.[5,11] For small R, the R group passes more easily through the annulus than the upper rim *tert*-butyl moiety. For large R, the passage of the R group is blocked and the *tert*-butyl substituent moves through the annulus. The latter process accounts for the maximum free energy barrier observed for large R. Contrary to the calix[4]arenes, the size of the calix[6]arene cavity is apparently large enough to allow the upper rim to move through the annulus, even when substituted with *tert*-butyl groups.

CHART 1

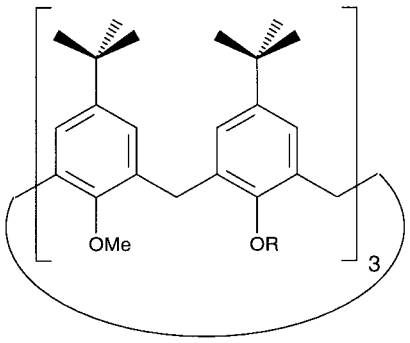

R	R
1a $CH_2C(O)NEt_2$	**1f** CH_2-(3-NO_2-C_6H_4)
1b CH_2-C_6H_5	**1g** CH_2-(3-CN-C_6-H_5)
1c $CH_2C(O)O$-*t*-Bu	**1h** CH_2-(2-naphtyl)
1d CH_2-(4-Br-C_6H_5)	**1i** CH_2-(4-C_6H_5-C_6H_4)
1e $PO(OEt)_2$	

The "upper rim through the annulus" mechanism has been postulated in order to explain the plateau of activation free energy reached with increasingly larger substituents R.[5,11] In this paper, the conformational interconversions of calix[6]arenes **1** are investigated with molecular modeling to test the *postulated* isomerization mechanisms. All calix[6]arenes **1** in Table 1 (except **1e**) contain a "O−CH_2−rigid group" motif. A variable-size atom Sx (S1−S10) is introduced to represent the substituents R, reducing the "O−CH_2−rigid group" motifs to one "O−CH_2−Sx" group. In this way the large number of degrees of freedom is reduced somewhat. The two possible Cone/1,2,3Alt isomerization pathways were compared for different sizes of Sx. It will be shown that the "upper rim through the annulus" mechanism is indeed plausible and that the observed maximum

S1089-5639(98)01201-8 CCC: $15.00
Published on Web 07/29/1998

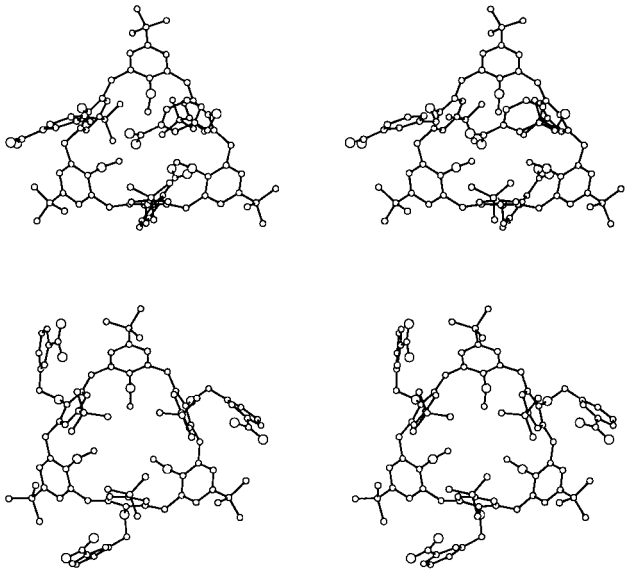

Figure 1. Major conformer Cone (lower) and minor conformer 1,2,-3Alt (upper) of **1** (hydrogen atoms not shown).

TABLE 1: Thermodynamic and Kinetic Parameters[5] for the Interconversion of Cone to 1,2,3Alt of Calix[6]arenes 1 in $CDCl_3$[a]

compound	$\Delta G°$	$\Delta G^{‡}$	compound	$\Delta G°$	$\Delta G^{‡}$
1a	1.7	20.8	**1f**	0.5	19.1
1b	0.7	16.7	**1g**	0.7	19.6
1c	1.4	18.7	**1h**	0.7	20.3
1d	0.5	20.6	**1i**	0.7	21.1
1e	1.0	19.1			

[a] $\Delta G°$ was measured at 303 K; $\Delta G^{‡}$, at 328 K. Both are given in kilocalories per mole.

free energy barrier for isomerism can be explained by the two competing interconversion pathways.

Experimental Section

Energy Minimizations. The energies of all conformations were minimized by the conjugate gradient followed by the Newton−Raphson method until the RMS (root-mean-square) value of the energy gradient was less than 10^{-12} kcal mol^{-1} Å^{-1}. For the evaluation of the energy and gradients, version 24b2 of the CHARMM[12] force field was used. A dielectric constant $\epsilon = 1$ was used with no cutoff for the nonbonded interactions. Energies and derivatives of **1** were evaluated with the parameters, partial charges, and energy function as used previously.[13] Two new united atoms (CH2E and Sx) were introduced for describing the 2,4,6 lower-rim substituent R (Chart 2 and Tables 2 and 3). The Sx atoms have been assigned no charge; the CH2E atom bears the total charge of the CH_3 atoms of an anisole ring. The Sx atoms have the same mass as a C atom. The parameter files of quanta[14] were adapted in order to produce graphical output with the S1−S10 atoms. Initial conformations were built from the Cone and 1,2,3-Alternate as calculated in ref 5. Saddle points were refined by minimizing the gradient of the energy until the RMS gradient was less than 10^{-12} kcal mol^{-1} Å^{-1}. The ∼AAA and ∼BBB conformations were built by setting the CA−CA−OE−CH2E dihedral (Chart 2) to 90° or −90°, respectively.

Normal Mode Calculation. All 3*N* (in which *N* is the number of atoms) modes were calculated. Each energy-minimized conformation was checked to be a true minimum by checking the absence of negative frequencies and the presence of six zero frequencies. The maximum deviation from zero was in the order of ≈0.2 cm^{-1}. The classical (ΔA_{cl}) and quantum mechanical (ΔA_{QM}) vibrational free energies as well as the zero-point correction energy (ΔA_0) were calculated:[15]

$$\Delta A_{QM} = kT\sum_{i=7}^{3N} \ln\left(1 - e^{-h\nu_i/kT}\right) \quad (1)$$

$$\Delta A_{cl} = kT\sum_{i=7}^{3N} \ln\left(\frac{h\nu_i}{kT}\right) \quad (2)$$

$$\Delta A_0 = \sum_{i=7}^{3N}\frac{h\nu_i}{2} \quad (3)$$

CHART 2. New Atom Types (CH2E and Sx) with Partial Charges for the Lower Rim 2,4,6-Substituents R of 1

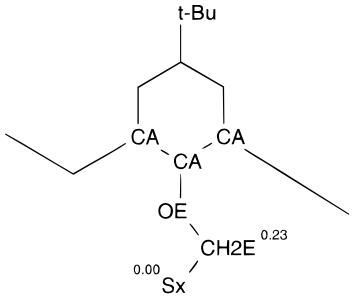

TABLE 2: Additional van der Waals Parameters

atom type	E_{min} (kcal mol^{-1})	$R_{min}/2$ (Å)	remarks
CH2E	−0.1142	2.235	CH2E parm19[a]
S1	−0.1811	2.165	CH3E parm19[a]
S2	−0.1811	2.3133	interpolated S1−S10
S3	−0.1811	2.4617	interpolated S1−S10
S4	−0.1811	2.6100	interpolated S1−S10
S5	−0.1811	2.7583	interpolated S1−S10
S6	−0.1811	2.9067	interpolated S1−S10
S7	−0.1811	3.0550	interpolated S1−S10
S8	−0.1811	3.2033	interpolated S1−S10
S9	−0.1811	3.3517	interpolated S1−S10
S10	−0.1811	3.500	long axis biphenyl ≈7 Å

[a] Parm19 is an older parametrization of charmm containing united atom models.

TABLE 3: Additional Bonded Parameters

bond	K_b (kcal mol^{-1} Å^{-2})	r_0 (Å)	remarks
CH2E−OE	296.70	1.45	= CT−OE
CH2E−S1	229.63	1.54	= CH2E−CH3E parm19[a]
CH2E−S2	229.63	2.1467	interpolated S1−S10
CH2E−S3	229.63	2.7533	interpolated S1−S10
CH2E−S4	229.63	3.3600	interpolated S1−S10
CH2E−S5	229.63	3.9667	interpolated S1−S10
CH2E−S6	229.63	4.5733	interpolated S1−S10
CH2E−S7	229.63	5.1800	interpolated S1−S10
CH2E−S8	229.63	5.7867	interpolated S1−S10
CH2E−S9	229.63	6.3933	interpolated S1−S10
CH2E−S10	229.63	7.0000	$r_0 = R_{min}$ vdW radius S10

angle	K_θ (kcal mol^{-1} rad^{-2})	θ_0 (deg)	
CA−OE−CH2E	110.0	109.7	= CA−OE−CT
OE−CH2E−Sx	75.7	110.1	= OH1−CT−CT

dihedral angle	K_ϕ (kcal mol^{-1})	ϕ (deg) [*n*]	
X−OE−CH2E−X	0.10	0.0 [3]	= HA−CT−OE−CA
CH2E−OE−CA−CA	1.40	180.0 [2]	= CA−CA−OE−CT

[a] Parm19 is an older parametrization of charmm containing united atom models.

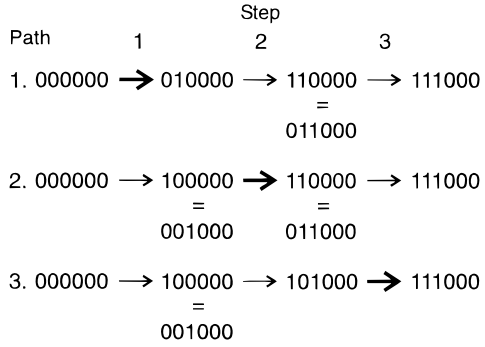

Figure 2. Six possible pathways for the 000000→111000 interconversion. Bold arrows denote rotation of the Sx-bearing ring, which can proceed in two ways: Sx or *t*-Bu through the annulus. Other arrows denote rotation of methoxy-bearing rings.

in which k is the Boltzmann constant, T is the temperature in kelvins, N is the number of atoms, h is the constant of Planck, and ν_i is the frequency of the ith mode.

Setup of Interconversion Pathways. The digits in the names of the conformations indicate which aromatic ring has been inverted. For instance: 000000 is a Cone, 111000 is a 1,2,-3Alt, 111111 is an inverted Cone, etc. In the 1,2,3Alt, either two rings bearing methoxy moieties and one ring bearing an Sx substituent have rotated with respect to the 000000 Cone (111000, 001110, or 100011), or one ring bearing a methoxy and two rings bearing Sx substituents (000111, 110001, or 011100).[16] The interconversion pathways of Cone → 1,2,3Alt of **1** can thus be divided in two groups of three equivalent paths. We assume that the rotation of a methoxy-bearing ring will not be rate-limiting when Sx is larger than methyl, and therefore we have calculated only the 000000 → 111000 pathway. In this pathway, two rings bearing a methoxy group have to rotate (rings 1 and 3), as well as one ring bearing Sx (ring 2). For the rotation of a methoxy-bearing ring, only the "methoxy through the annulus" path is considered. The Sx-bearing ring can rotate with either Sx or *t*-Bu through the annulus, so that a total of six pathways have been taken into account (Figure 2). To vary the start and final conformations of the reaction path calculations, the CH2E atoms of the 2,4,6-substituents are made pointing outward (indicated with ∼AAA) or inward (indicated with ∼BBB) with respect to the annulus. This doubles the number of interconversion pathways, because all interconversion steps were calculated with both the ∼AAA and ∼BBB conformers. Combinations of inward and outward positions are also possible, but they were not considered in order to save computational efforts. The radius of Sx was varied in 10 steps from 4.33 Å (S1: CH_3 extended atom) to 7.0 Å (S10: ≈ largest C−C distance in a biphenyl unit). For each size of Sx, the lowest free energy transition state was determined for Sx or *t*-Bu through the annulus pathways. A total of 200 interconversions have been calculated. Free energy barriers were calculated with respect to the global lowest free energy conformation for each Sx substituent.

Reaction Path Calculations. The conjugate peak refinement (CPR) algorithm[17−19] searches for maxima along the adiabatic energy valley connecting two local minima on an adiabatic energy surface. These maxima are refined to saddle points and represent the transition states of the reaction pathway between the two minima. All the degrees of freedom of the molecule can contribute to the reaction path. There is no need at all to choose a reduced reaction coordinate such as a rotation around a certain bond. The algorithm has been integrated into CHARMM[12,15] in the TRAVEL module. First, all the interconversions with the smallest Sx (S1) were calculated. As an initial guess, three intermediates were provided in which the aromatic ring was rotated 45, 90, and 135°, respectively, around the axis connecting the C-atoms ortho to the lower rim substituent. In all intermediates, the three methoxy moieties were rotated out of the cavity to make way for the rotating aromatic ring. The output of these calculations was used as initial guess for the calculations with the smallest one but Sx (S2), etc. The CPR method at first interpolates linearly between the Cartesian coordinates of the reactant, the product, and the initial intermediates. In a number of cases, these interpolations result in a path with some nonphysical segments. In the case of **1**, methyl groups often inverted like umbrellas during a storm. This problem was resolved by deleting all hydrogens in such a trajectory and rebuilding them from internal coordinates, followed by further refinement of the trajectory by CPR. Only the highest saddle point in each trajectory was fully refined to save computational efforts.

Results and Discussion

Energy Minimizations. All free energies in this paper were calculated including the quantum mechanical or the classical vibrational contributions. Since the differences between these contributions were small and in no case influenced the relative order of minimized conformers (or transition states), only free energies including the quantum mechanical contributions are discussed. Selected results of energy minimizations and normal mode calculations are presented in Table 4. Intermediate conformations of the 000000 → 111000 pathway (Figure 2) were also minimized but are not shown, since our primary interest was in the transition states connecting 000000 with 111000, not in the conformational distribution of calix[6]arene **1**. For all sizes of Sx, the 111000∼ABB was the lowest potential energy conformer. However, when the vibrational free energy was taken into account, the 000000∼AAA was the most favorable conformer (Figure 4). This is in agreement with previous experimental findings[5] that the Cone is the major conformer and the 1,2,3Alt is the minor (Table 1). In the Cone conformation the three OMe groups are filling the cavity, which is consistent with experimental data.[5] This stabilization of the Cone will be the result of favorable van der Waals and/or electrostatic interactions, without the need of introducing "magic" forces (vide infra). The free energy of the Cone as a function of the radius of the Sx group was not constant but varied (Figure 3).

The maximum difference is 3.4 kcal mol^{-1} between calix[6]arene **1** with S3 substituents (0.5 kcal mol^{-1}) and with S10 substituents (−2.9 kcal mol^{-1}). An explanation for the maximum free energy for S3 substituents can be found in Figure 4, where all of the calix[6]arene but the Sx atoms are overlapping. The Cone of calix[6]arene **1** having S3 substituents is the only conformer in Figure 4 having all three C_{aro}−O−CH2E−S3 dihedral angles (Chart 2) deviate from the optimal 180°.

Isomerizations. The free energies of the rate-limiting transition states of both isomerization mechanisms are presented in Table 5 and Figure 3. The free energy barrier for the "*t*-Bu through the annulus" mechanism is reasonably constant, with a minimum of 15.7 kcal mol^{-1} for S10 and a maximum of 17.8 kcal mol^{-1} for S3−S5. This isomerization barrier was expected to be nearly constant, since the *tert*-butyl moiety that passes through the annulus is in all cases the same. There was not much free energy difference when using either of the ∼AAA and ∼BBB start and final conformations. The calculated isomerization barriers indicate that the postulated "*t*-Bu through

TABLE 4: Normalized Results of Energy Minimizations and Vibrational Free Energy Calculations[a] of Selected Conformers of 1 at $T = 300$ K

conformation	Sx	R_{min} (Å)	n	E_{min}	ΔA_{qm}	ΔA_{cl}	ΔA_0	ΔA_{total} QM	ΔA_{total} cl
000000∼AAA	S1	4.33	2	4.1	−4.3	−5.3	−1.4	0.5	0.6
000000∼BBB	S1	4.33	2	3.0	−3.9	−4.8	−1.1	0.0	0.0
111000∼BAA	S1	4.33	6	0.9	−1.6	−1.9	−0.4	0.3	0.1
111000∼ABB	S1	4.33	6	0.0	0.0	0.0	0.0	1.4	1.1
000000∼AAA	S2	4.63	2	4.4	−5.9	−7.2	−1.7	−1.2	−1.0
000000∼BBB	S2	4.63	2	3.3	−4.5	−5.5	−1.4	−0.5	−0.4
111000∼BAA	S2	4.63	6	1.2	−1.7	−2.2	−0.8	0.1	0.1
111000∼ABB	S2	4.63	6	0.4	−0.1	−0.4	−0.4	1.3	1.2
000000∼AAA	S3	4.92	2	4.6	−4.5	−5.8	−1.8	0.5	0.7
000000∼BBB	S3	4.92	2	3.5	−3.3	−4.4	−1.5	0.8	1.0
111000∼BAA	S3	4.92	6	1.5	−2.0	−2.7	−1.0	0.0	0.0
111000∼ABB	S3	4.92	6	0.9	−0.6	−1.0	−0.6	1.2	1.1
000000∼AAA	S4	5.22	2	4.9	−5.9	−7.3	−1.9	−0.8	−0.6
000000∼BBB	S4	5.22	2	3.6	−3.4	−4.5	−1.5	0.7	0.8
111000∼BAA	S4	5.22	6	1.7	−2.2	−3.0	−1.1	−0.2	−0.1
111000∼ABB	S4	5.22	6	1.3	−1.0	−1.5	−0.7	1.0	0.9
000000∼AAA	S5	5.52	2	5.6	−8.1	−9.8	−2.3	−2.6	−2.4
000000∼BBB	S5	5.52	2	3.7	−4.8	−6.0	−1.7	−0.6	−0.5
111000∼BAA	S5	5.52	6	1.8	−2.4	−3.2	−1.1	−0.3	−0.3
111000∼ABB	S5	5.52	6	1.4	−1.0	−1.6	−0.8	1.0	0.9
000000∼AAA	S6	5.81	2	5.9	−8.0	−9.8	−2.3	−2.4	−2.1
000000∼BBB	S6	5.81	2	3.4	−4.5	−5.8	−1.7	−0.7	−0.6
111000∼BAA	S6	5.81	6	1.8	−2.6	−3.5	−1.2	−0.6	−0.6
111000∼ABB	S6	5.81	6	1.5	−1.4	−2.0	−0.8	0.7	0.7
000000∼AAA	S7	6.11	2	6.0	−8.2	−10.0	−2.4	−2.4	−2.2
000000∼BBB	S7	6.11	2	4.0	−5.4	−6.8	−1.9	−1.2	−1.0
111000∼BAA	S7	6.11	6	1.7	−2.9	−3.8	−1.2	−1.0	−0.9
111000∼ABB	S7	6.11	6	1.6	−1.7	−2.3	−0.9	0.4	0.4
000000∼AAA	S8	6.41	2	6.1	−8.4	−10.2	−2.4	−2.6	−2.2
000000∼BBB	S8	6.41	2	3.8	−5.5	−6.9	−1.9	−1.5	−1.3
111000∼BAA	S8	6.41	6	2.9	−4.4	−5.5	−1.4	−1.5	−1.5
111000∼ABB	S8	6.41	6	2.8	−3.3	−4.1	−1.1	−0.1	−0.2
000000∼AAA	S9	6.70	2	6.2	−8.6	−10.4	−2.4	−2.7	−2.4
000000∼BBB	S9	6.70	2	3.7	−5.6	−7.1	−1.9	−1.8	−1.6
111000∼BAA	S9	6.70	6	3.0	−4.6	−5.7	−1.5	−1.6	−1.5
111000∼ABB	S9	6.70	6	3.0	−3.5	−4.3	−1.1	−0.1	−0.2
000000∼AAA	S10	7.00	2	6.3	−8.8	−10.7	−2.5	−2.9	−2.6
000000∼BBB	S10	7.00	2	3.6	−5.8	−7.3	−2.0	−2.1	−1.9
111000∼BAA	S10	7.00	6	3.2	−4.9	−6.0	−1.5	−1.8	−1.7
111000∼ABB	S10	7.00	6	3.2	−3.7	−4.6	−1.1	−0.3	−0.3

[a] Energies are given in kilocalories per mole.

the annulus" mechanism is indeed feasible. In all cases but one, the position of the rate-limiting step is the 100000 → 110000 conversion. The exception is found for S10, where the rate-limiting step 101000 → 111000 is favored by only 0.2 kcal mol^{-1} over the 100000 → 110000 conversion. The free energy barriers for the 100000 → 110000 conversions are comparable (within 1.5 kcal mol^{-1}) to the barriers of the 101000 → 111000 conversions, while the 000000 → 100000 steps have considerably higher free energy barriers (≈7 kcal mol^{-1} higher). A "*tert*-butyl through the annulus" step is apparently sterically more hindered in the first step of the Cone → 1,2,3Alt isomerization than in either the second or third step (pathways 2 and 3 in Figure 2). The similarity of the rate-limiting "*t*-Bu through the annulus" transition states is clear in Figure 5, which shows that almost all variation is found in the positions of the Sx groups.

For the "Sx through the annulus" mechanism, the free energy of the saddle points is expected to increase for larger Sx. The increase will not be linear since the van der Waals interaction function, which dominates the transition-state energy for larger Sx, contains $1/r^6$ and $1/r^{12}$ terms and is therefore highly nonlinear. The lower rim substituent has three rotatable bonds, while the *tert*-butyl moiety has essentially only the phenyl−butyl bond (not counting rotations around the C−Me bonds). The conformational freedom of the Sx group is therefore larger, and the variation in the saddle point energies is expected to vary more than is the case with the *tert*-butyl moving through the annulus. This variation is indeed found. For instance, the differences between the calculated barriers starting from the ∼AAA of ∼BBB Cone conformers were larger than was the case for the "*tert*-butyl through the annulus" mechanism. For Sx ≤ S3, the free energy barriers are comparable to the barriers of the "methoxy through the annulus" mechanism. In fact, the rate-limiting barriers for S1 and S2 are rotations of methoxy moieties between inside and outside positions. The initial guesses for the travel calculations with S1 had their methoxy

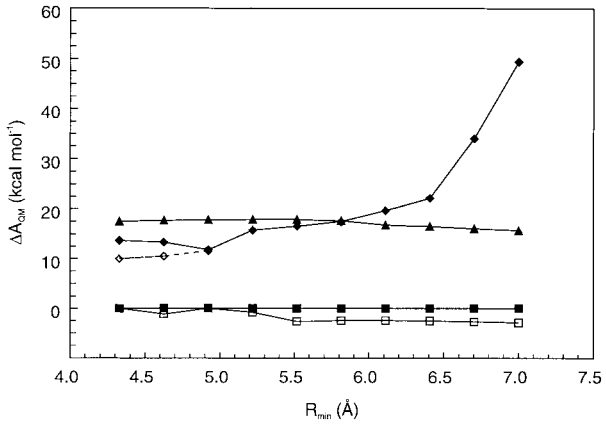

Figure 3. Free energy (including quantum chemical vibrational contribution) as a function of the van der Waals radius R_{min} of the lower rim 2,4,6 substituents Sx. Solid diamonds indicate the free energy barriers of the "Sx through the annulus" pathway, and triangles indicate the "*tert*-butyl through the annulus" pathway. Open diamonds are the free energy barriers of true "Sx through the annulus" rotations (see text). Open squares indicate the free energy of the minimized 000000∼AAA conformers normalized to $R_{min} = 4.33$ Å. Solid squares are the free energies of the 000000∼AAA conformers, each normalized to $\Delta A_{total} = 0$ kcal mol^{-1}, which were used as reference states for the free energy barriers of all isomerizations.

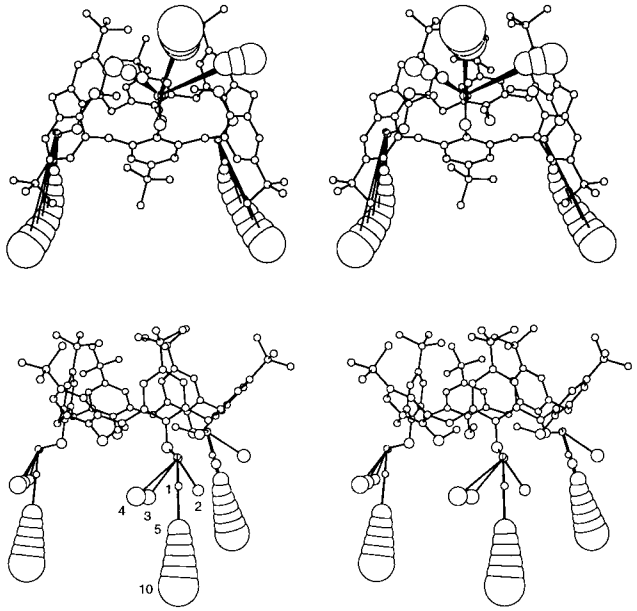

Figure 4. Energy-minimized 111000∼BAA (upper) and 000000∼AAA (lower) conformations with lower rim substituents S1−S10. Hydrogen atoms are not shown for clarity.

TABLE 5: Free Energy Barriers of Both Isomerism Pathways of 1 as a Function of the Radius of the Lower Rim Substituent Sx[a]

Sx	R_{min} (Å)	$\Delta A^{\ddagger}$(OSx)	path (step)	$\Delta A^{\ddagger}$(*t*-Bu)	path (step)
S1	4.33	**13.6**	3 (3)∼BBB	17.5	2 (2)∼BBB
S2	4.63	**13.3**	3 (3)∼BBB	17.6	2 (2)∼BBB
S3	4.92	**11.8**	2 (1)∼BBB	17.8	2 (2)∼BBB
S4	5.22	**15.7**	3 (3)∼AAA	17.8	2 (2)∼BBB
S5	5.52	**16.5**	2 (2)∼AAA	17.8	2 (2)∼BBB
S6	5.81	**17.5**	3 (3)∼AAA	**17.6**	2 (2)∼AAA
S7	6.11	19.6	3 (3)∼AAA	**16.7**	2 (2)∼BBB
S8	6.41	22.1	1 (1)∼AAA	**16.5**	2 (2)∼BBB
S9	6.70	34.0	1 (1)∼AAA	**16.0**	2 (2)∼AAA
S10	7.00	49.4	1 (1)∼AAA	**15.7**	3 (3)∼AAA

[a] $\Delta A^{\ddagger}$(OSx) and $\Delta A^{\ddagger}$(t-Bu) are free energy barriers (including quantum mechanical vibrational contribution) in kilocalories per mole of the "Sx group through the annulus" and "*tert*-butyl through the annulus" mechanisms, respectively. path (step) denotes where the rate-limiting step can be found in Figure 2. The free energies shown in boldface type denote the preferred pathway of the two considered isomerization processes.

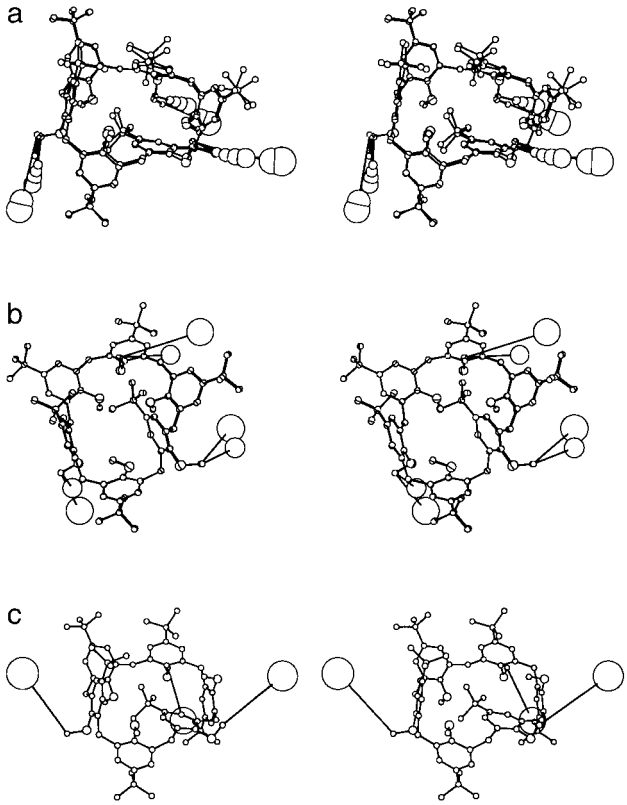

Figure 5. Transition-state conformations of the "*tert*-butyl through the annulus" mechanism with lower rim substituents S1−S5 and S7−S8 (top), S6 and S9 (middle), and S10 (bottom). Hydrogen atoms are not shown for clarity.

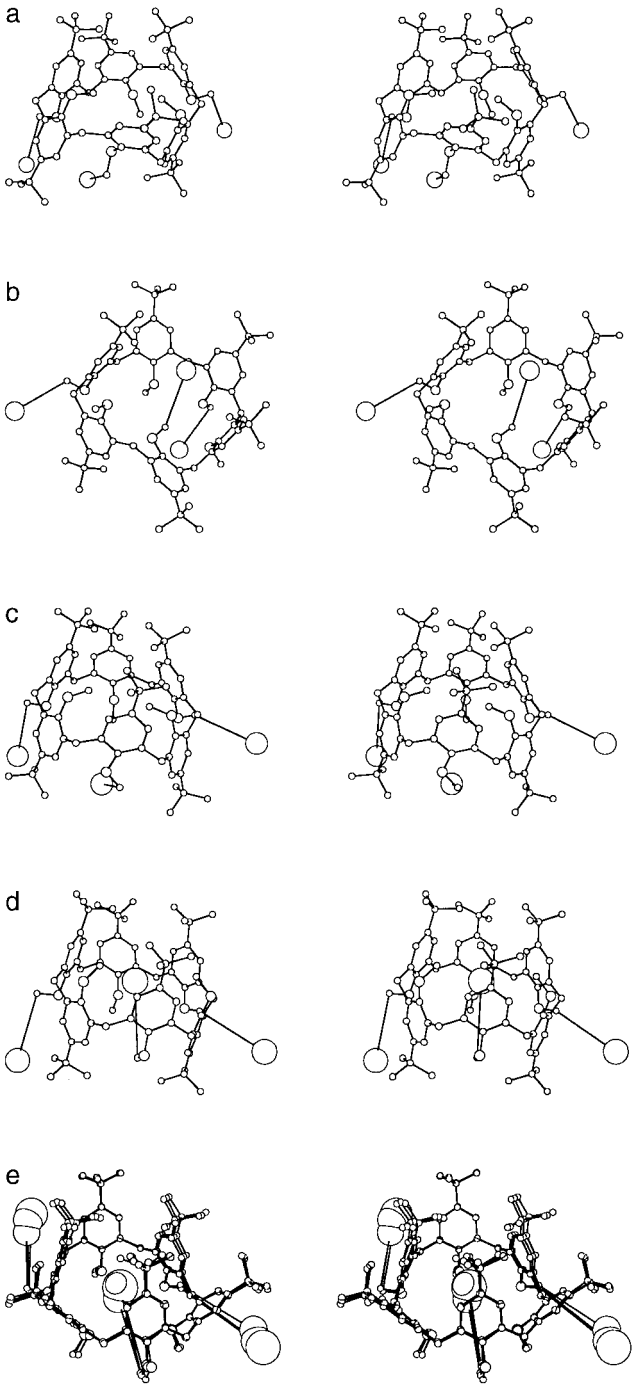

Figure 6. Transition-state conformations with lower rim substituents S4 (top) to S6 (bottom) of the "Sx through the annulus" mechanism. Hydrogen atoms are not shown for clarity.

groups rotated outside the annulus because this enlarges the free diameter of the annulus and lowers the energy barrier for the rotations of larger Sx. Since the output trajectories of the calculations with Sx were input for the calculations with Sx + 1, already for S1 the methoxy groups had to rotate to outside positions. For S3, the rate-limiting interconversion is a "methoxy through the annulus" step. The dotted line in Figure 3 shows the free energy barrier of the "Sx through the annulus" mechanism calculated when only the rotations of the Sx-bearing rings were taken into account. For Sx ≤ S6, the Sx group is still smaller than the diameter of the annulus. In Figure 6 the rate-limiting steps for Sx = S4−S6 are shown. For these sizes of Sx, the Sx group of the rotating ring either has already passed or still has to pass the smallest diameter of the annulus. The passage of the Sx group through the annulus is not rate-limiting, but the rearrangements to put the Sx group in the center of the annulus before or after the passage. Only when Sx > S6 the passage of the Sx group through the annulus becomes rate-limiting, as can be seen in Figure 6. The Sx group is located at the smallest diameter of the annulus, as expected if the steric hindering of the passage of this group is rate-limiting. The $C_{aro}-O-CH2E-Sx$ dihedral angles (Chart 2) of the rotating ring are all ≈0°, allowing the Sx group to pass exactly through the center of the annulus. The calix[6]arenes **1** used in experiments (Table 1)[5] had a similar "$O-CH_2-$rigid group" motif as the $O-CH_2-Sx$ used in the calculations. Therefore, we predict that the "Sx through the annulus" interconversions

of calix[6]arenes **1** proceed via a similar folding, which allows the rigid substituent to pass through the center of the annulus. We also predict that without the CH_2 spacer, the ability will be reduced of positioning the Sx group at the center of the annulus, and the isomerization barrier will be increased.

The Preferred Pathway. For Sx = S6 (5.81 Å), the barriers of both isomerization mechanisms are equal within 0.1 kcal mol^{-1}. The calculated free energy barriers for the "*tert*-butyl through the annulus" mechanism show a standard deviation of 0.8 kcal mol^{-1}. This free energy barrier is expected to be constant, so this number is used as an estimation of the variation in the calculated free energies. With this variation, the graphs of the "*tert*-butyl through the annulus" and "Sx through the annulus" intersect between S5 and S6. Because only for Sx ≥ S7 does the passage of the Sx group through the annulus become rate-limiting in the "Sx through the annulus" pathway, we conclude that the "*tert*-butyl through the annulus" becomes preferred for Sx ≥ S7 (6.11 Å). The calculated free energy limit for the Cone → 1,2,3Alt interconversion barrier is 17.5 kcal mol^{-1}. This number is reasonably close to the experimental 21 kcal mol^{-1}, given the crude model of one uncharged atom of variable size as model for a range of lower-rim substituents and the neglect of solvent effects. However, we do not expect significant solvent effects in chloroform because 1,3,5-trimethoxycalix[6]arenes do not possess a real cavity that can be stabilized by solvent inclusion. In addition to this, a recent theoretical study on tetramethoxycalix[4]arene showed that dichloromethane is able to stabilize the cone with respect to the other conformations, but chloroform is not.[20]

Conclusions

The present study shows that the postulated competing mechanisms of Cone → 1,2,3Alt isomerization, the "*tert*-butyl through the annulus" and "Sx through the annulus" pathways, are indeed plausible. For large lower-rim substituents (Sx ≥ ≈6 Å), the "*tert*-butyl through the annulus" mechanism is preferred over the "Sx through the annulus" mechanism. The calculated upper free energy barrier for the isomerization process is 17.5 kcal mol^{-1}, reasonably close to the experimental value of approximately 21 kcal mol^{-1}. The successful calculations on systems with many degrees of freedom is encouraging and can be useful to steer the future design of fixed conformations.

References and Notes

(1) (a) Gutsche, C. D. *Calixarenes*; Royal Society of Chemistry: Cambridge, England, 1989. (b) *Calixarenes; A Versatile Class of Compounds*; Vicens, J., Böhmer, V., Eds.; Kluwer Academic Publishers: Dordrecht, The Netherlands, 1991. (c) Böhmer, V. *Angew. Chem., Int. Ed. Engl.* **1995**, *34*, 713. (d) Pochini, A.; Ungaro, R. *Comprehensive Supramolecular Chemistry*; Vögtle, F., Ed.; Elsevier: Oxford, England, 1996; Vol. 2, pp 103−142.

(2) (a) Kanamathareddy, S.; Gutsche, C. D. *J. Org. Chem.* **1994**, *59*, 3871. (b) Otsuka, H.; Araki, K.; Shinkai, S. *J. Org. Chem.* **1994**, *59*, 1542. (c) Neri, P.; Rocco, C.; Consoli, G. M. L.; Piattelli, M. *J. Org. Chem.* **1993**, *58*, 6535. (d) Neri, P.; Foti, M.; Ferguson, G.; Gallagher, J. F.; Kaitner, B.; Pons, M.; Molins, M. A.; Giunta, L.; Pappalardo, S. *J. Am. Chem. Soc.* **1992**, *114*, 7814. (e) Janssen, R. G.; Verboom, W.; Harkema, S.; van Hummel, G. J.; Reinhoudt, D. N.; Pochini, A.; Ungaro, R.; Prados, P.; de Mendoza, J. *J. Chem. Soc., Chem. Commun.* **1993**, 506. (f) Janssen, R. G.; van Duynhoven, J. P. M.; Verboom, W.; van Hummel, G. J.; Harkema, S.; Reinhoudt, D. N. *J. Am. Chem. Soc.* **1996**, *118*, 3666. (g) Janssen, R. G.; Verboom, W.; Reinhoudt, D. N.; Casnati, A.; Freriks, M.; Pochini, A.; Ugozolli, F.; Ungaro, R.; Nieto, P. M.; Carramolino, M.; Cuevas, F.; Prados, P.; de Mendoza, J. *Synthesis* **1993**, 380. (h) Moran, J. K.; Georgiev, E. M.; Yordanov, A. T.; Mague, J. T.; Roundhill, D. M. *J. Org. Chem.* **1994**, *59*, 5990.

(3) Rogers, J. S.; Gutsche, C. D. *J. Org. Chem.* **1992**, *57*, 3152.

(4) Ahn, S.; Lee, J. W.; Chang, S.-K. *J. Chem. Soc., Perkin Trans. 2* **1996**, 79.

(5) van Duynhoven, J. P. M.; Janssen, R. G.; Verboom, W.; Franken, S. M.; Casnati, A.; Pocini, A.; Ungaro, R.; de Mendoza, J.; Nieto, P. M.; Prados, P.; Reinhoudt, D. N. *J. Am. Chem. Soc.* **1994**, *116*, 5814.

(6) Kanamathareddy, S.; Gutsche, C. D. *J. Am. Chem. Soc.* **1993**, *115*, 6572.

(7) Otsuka, H.; Shinkai, S. *J. Am. Chem. Soc.* **1996**, *118*, 4271.

(8) Janssen, R. G.; Verboom, W.; van Duynhoven, J. P. M.; van Velzen, E. J. J.; Reinhoudt, D. N. *Tetrahedron Lett.* **1994**, *35*, 6555.

(9) (a) Araki, K.; Akao, K.; Otsuka, H.; Nakashima, K.; Inokuchi, F.; Shinkai, S. *Chem. Lett.* **1994**, 1251. (b) Otsuka, H.; Araki, K.; Matsumoto, H.; Harada, T.; Shinkai, S. *J. Org. Chem.* **1995**, *60*, 4862.

(10) Casnati, A.; Minari, P.; Ungaro, R. *J. Chem. Soc., Chem. Commun.* **1991**, 1413.

(11) (a) Otsuka, H.; Araki, K.; Sakaki, T.; Nakashima, K.; Shinkai, S. *Tetrahedron Lett.* **1993**, *45*, 7275. (b) Otsuka, H.; Araki, K.; Shinkai, S. *Chem. Express* **1993**, *8*, 479.

(12) Brooks, B. R.; Bruccoleri, R. E.; Olafson, B. D.; States, D. J.; Swaminathan, S.; Karplus, M. *J. Comput. Chem.* **1983**, *4*, 187.

(13) (a) Fischer, S.; Grootenhuis, P. D. J.; Groenen, L. C.; van Hoorn, W. P.; van Veggel, F. C. J. M.; Reinhoudt, D. N.; Karplus, M. *J. Am. Chem. Soc.* **1995**, *117*, 1611. (b) van Hoorn, W. P.; Morshuis, M. G. H.; van Veggel, F. C. J. M.; Reinhoudt, D. N. *J. Phys. Chem. A* **1998**, *102*, 1130.

(14) QUANTA version 4.1; Molecular Simulations Inc.: Waltham, MA, 1995.

(15) Brooks, B. R.; Janežič, D.; Karplus, M. *J. Comput. Chem.* **1995**, *12*, 1522.

(16) Note that all six 1,2,3-Alternate conformations are equivalent.

(17) Fischer, S.; Karplus, M. *Chem. Phys. Lett.* **1992**, *194*, 252.

(18) (a) Fischer, S.; Michnick, S.; Karplus, M. *Biochemistry*, **1993**, *32*, 13830. (b) Fischer, S.; Dunbrack, R. L., Jr.; Karplus, M. *J. Am. Chem. Soc.* **1994**, *116*, 11931. (c) Verma, C. S.; Fischer, S.; Caves, L. S. D.; Roberts, G. C. K.; Hubbard, R. E. *J. Phys. Chem.* **1996**, *100*, 2510.

(19) van Hoorn, W. P.; van Veggel, F. C. J. M.; Reinhoudt, D. N. *J. Org. Chem.* **1996**, *61*, 7180.

(20) van Hoorn, W. P.; Briels, W. J.; van Duynhoven, J. P. M.; van Veggel, F. C. J. M.; Reinhoudt, D. N. *J. Org. Chem.* **1998**, *63*, 1299.